Characterization of Highly Ordered MCM-41 Silicas Using X-ray Diffraction and Nitrogen Adsorption

Michal Kruk and Mietek Jaroniec*

Department of Chemistry, Kent State University, Kent, Ohio 44240

Ji Man Kim and Ryong Ryoo

Department of Chemistry and Center for Molecular Science, Korea Advanced Institute of Science and Technology, Taeduk Science Town, Taejon, 305-701 Korea

Received February 18, 1999. In Final Form: May 5, 1999

Highly ordered MCM-41 silicas were synthesized in the presence of alkyltrimethylammonium surfactants and characterized using powder X-ray diffraction and nitrogen adsorption at 77 K. Samples prepared in the presence of hexadecyltrimethylammonium ($HTMA^+$) and octadecyltrimethylammonium surfactants using the repeated pH adjustment method were found to exhibit a very high degree of structural ordering and (100) interplanar spacings of 4.1 and 4.6 nm, respectively. Using a high-temperature (438 K) synthesis procedure involving $HTMA^+$ surfactants, it was also possible to prepare MCM-41 with the (100) spacing above 5 nm, which exhibited as many as five distinct XRD peaks. The MCM-41 materials had appreciable amounts of secondary mesopores, but no micropores. Pore sizes evaluated from (100) interplanar spacings and primary mesopore volumes using geometrical considerations were found to be in excellent agreement with those calculated using the Barrett−Joyner−Halenda method with the recently reported modified version of the Kelvin equation for nitrogen adsorption in cylindrical pores. Statistical film thickness curves (*t* curves) for nitrogen adsorbed on the surface of MCM-41 pores were also evaluated and compared with the *t* curve for a macroporous silica gel. It was shown that although all these *t* curves were very similar to one another in the low-pressure range, the statistical film thickness for MCM-41 was slightly enhanced as the primary mesopore size decreased. At higher pressures, an increase in the statistical film thickness was observed as the capillary condensation pressure range was approached, especially for the material with the smallest primary mesopore diameter. Thus, the current study of highly ordered MCM-41 materials demonstrates a self-consistency of pore size analysis methods based on geometrical considerations and on the modified Kelvin equation.

Introduction

Discovery of ordered mesoporous materials,[1,2] and MCM-41 in particular,[1] opened new opportunities in gas adsorption. MCM-41 with hexagonally ordered arrays of long, approximately cylindrical pores was immediately recognized as an excellent model adsorbent.[3−6] However, the range of pore sizes attainable for good-quality MCM-41 was initially limited to about 4.5 nm. This upper boundary of the pore diameter coincides with a lower pore size limit of occurrence of adsorption−desorption hysteresis in the case of the most commonly used experimental conditions (that is, nitrogen adsorption at 77 K), further complicating adsorption data analysis.[4] Synthesis procedures for well-ordered large-pore MCM-41 (pore diameter above 4.5 nm) have been developed recently, and the upper limit of accessible pore sizes was extended to at least 7 nm.[2,7−10] This in turn allowed for preparation of MCM-41 materials in a wide range of pore diameters and their subsequent use to test the validity of the Kelvin equation.[11] A modified form of the Kelvin equation for nitrogen adsorption in cylindrical pores was proposed and the nitrogen statistical film thickness curve (*t* curve) for silicas was also derived.[11] However, in the original study,[11] the number of model MCM-41 materials used was limited, especially in the pore size region of the transition from adsorption−desorption behavior not accompanied with hysteresis to the one accompanied with hysteresis. The aim of the current study was to synthesize highly ordered MCM-41 materials, to characterize their structural properties, and to use them to further examine the validity of (i) the corrected form of the Kelvin equation and (ii) the *t* curve for mesoporous silicas.

Materials and Methods

Materials. Pure-silica MCM-41 materials with various (100) interplanar spacings between 3.4 and 5.4 nm were prepared following two hydrothermal synthesis procedures reported previously.[9,12,13] Briefly, three MCM-41 materials with $3.4 < d_{100}$

* To whom correspondence should be addressed. E-mail: Jaroniec@scorpio.kent.edu. Phone: (330)672 3790. Fax: (330)672 3816.

(1) Beck, J. S.; Vartuli, J. C.; Roth, W. J.; Leonowicz, M. E.; Kresge, C. T.; Schmitt, K. D.; Chu, C. T−W.; Olson, D. H.; Sheppard, E. W.; McCullen, S. B.; Higgins, J. B.; Schlenker, J. L. *J. Am. Chem. Soc.* **1992**, *114*, 10834.

(2) Huo, Q.; Margolese, D. I.; Stucky, G. D. *Chem. Mater.* **1996**, *8*, 1147.

(3) Franke, O.; Schulz-Ekloff, G.; Rathousky, J.; Starek, J.; Zukal, A. *J. Chem. Soc., Chem. Commun.* **1993**, 724.

(4) Branton, P. J.; Hall, P. G.; Sing, K. S. W.; Reichter, H.; Schuth, F.; Unger, K. K. *J. Chem. Soc., Faraday Trans.* **1994**, *90*, 2965.

(5) Ravikovitch, P. I.; Haller G. L.; Neimark, A. V. *Adv. Colloid Interface Sci.* **1998**, *76−77*, 203.

(6) Morishige, K.; Fujii, H.; Uga, M.; Kinukawa, D. *Langmuir* **1997**, *13*, 3494.

(7) Khushalani, D.; Kuperman, A.; Ozin, G. A.; Tanaka, K.; Garces, J.; Olken, M. M.; Coombs, N. *Adv. Mater.* **1995**, *7*, 842.

(8) Sayari, A.; Liu, P.; Kruk, M.; Jaroniec, M. *Chem. Mater.* **1997**, *9*, 2499.

(9) Cheng, C.-F.; Zhou, W.; Park, D. H.; Klinowski, J.; Hargreaves, M.; Gladden, L. F. *J. Chem. Soc., Faraday Trans.* **1997**, *93*, 359.

(10) Corma, A.; Kan, Q.; Navarro, M. T.; Perez-Pariente, J.; Rey, F. *Chem. Mater.* **1997**, *9*, 2123.

(11) Kruk, M.; Jaroniec, M.; Sayari A. *Langmuir* **1997**, *13*, 6267.

(12) Ryoo, R.; Kim, J. M. *J. Chem. Soc., Chem. Commun.* **1995**, 711.

10.1021/la990179v CCC: $18.00
Published on Web 06/15/1999

< 4.6 nm were synthesized using an aqueous solution of sodium silicate (Na/Si = 0.5)[12,13] as a silica source at 373 K and alkyltrimethylammonium halides ($C_nH_{2n+1}N(CH_3)_3X$, $n = 12$, 16, and 18, and X = Cl for $n = 16$, and Br for $n = 12$ and 18) as surfactants. The starting materials were mixed at room temperature to give a gel composition of 4/1/1/250, SiO_2/surfactant/Na_2O/H_2O.[12,13] The starting mixture was heated at 373 K for 4 days. During the reaction period at 373 K, the mixture was cooled to room-temperature three times and acetic acid was added to adjust the pH to 10. The resultant surfactant−silica mesophase was filtered, washed with distilled water, dried at 393 K, washed with an ethanol−HCl mixture, and calcined in ambient air conditions at 813 K.[12,13] The calcined samples are designated MCM-41-12, MCM-41-16A, and MCM-41-18, respectively. Two additional MCM-41 materials with $d_{100} = 5.04$ and 5.37 nm were synthesized using Aerosil 200 (Degussa) as a silica source and hexadecyltrimethylammonium bromide as a surfactant. The gel composition used in these syntheses was 1/0.19/0.27/40, SiO_2/tetramethylammonium hydroxide/surfactant/H_2O.[9] The hydrothermal synthesis was performed at 438 K for 2 and 5 days, producing samples designated as MCM-41-16B and MCM-41-16C, respectively. The surfactant was removed from the samples, following the same ways used for the above smaller pore materials.

Measurements. Powder X-ray diffraction patterns were acquired on a Rigaku D/MAX-III instrument using Cu Kα radiation. Nitrogen adsorption measurements were performed on an ASAP 2010 volumetric adsorption analyzer manufactured by Micromeritics (Norcross, GA). Before measurements, the samples were outgassed for 2 h at 473 K in the degas port of the adsorption analyzer.

Calculation Procedures. BET specific surface areas[14] for the materials under study were evaluated using nitrogen adsorption data in the relative pressure range from 0.04 to 0.2, with the exception of MCM-41-12, for which the interval from 0.04 to 0.1 was used. The total pore volume was estimated on the basis of the amount adsorbed at the relative pressure of about 0.99. The external surface area and the primary mesopore volume were evaluated using the a_s plot method[3,4,8,13,14] in the a_s range from 1.3 to 1.8 for the samples MCM-41-12, -16A, and -18 and from 1.6 to 2.4 for samples MCM-41-16B and -16C (a_s is the standard reduced adsorption defined as a ratio of the adsorbed amount to the adsorbed amount at the relative pressure of 0.4). Low-pressure data in the a_s range from 0 to 0.7 (or from 0 to 0.6 in the case of sample MCM-41-12) were examined to prove the absence of microporosity.[8,11,13] A macroporous silica gel LiChrospher Si-1000 was used as a reference adsorbent in the a_s plot method.[8,13]

The primary mesopore diameter, w_d, was evaluated using the following equation derived for materials with hexagonal arrays of uniform pores:[11,15]

$$w_d = cd_{100}\left(\frac{\rho V_p}{1+\rho V_p}\right)^{1/2} \tag{1}$$

where c is a constant (equal to 1.213 in the case of circular pore geometry), d_{100} is the (100) interplanar spacing, ρ is the pore wall density (assumed to be 2.2 g/cm^3), and V_p is the primary mesopore volume. Circular pore geometry was assumed. The pore wall thickness, b_d, was estimated as the distance between pore centers, a ($a = 2/3^{1/2}d_{100}$) minus the primary mesopore size, $b_d = a - w_d$.[8,13]

Mesopore size distributions for the materials under study were evaluated from adsorption branches of nitrogen isotherms using the Barrett−Joyner−Halenda (BJH) method[16] with the corrected Kelvin equation for nitrogen adsorption in cylindrical pores:[11]

$$r(p/p_0)\ [\text{nm}] = \frac{2\gamma V_L}{RT\ln[p_0/p]} + t(p/p_0) + 0.3 \tag{2}$$

where p is the equilibrium vapor pressure, p_0 is the saturation vapor pressure, p/p_0 is the relative pressure, $r(p/p_0)$ is the pore radius as a function of the relative pressure, γ and V_L are the surface tension and the molar volume of liquid nitrogen at 77 K, R is the universal gas constant, T is the absolute temperature, and t is the statistical film thickness (t curve) for nitrogen adsorbed on the pore walls. The t curve was based on the adsorption isotherm for a macroporous silica gel LiChrospher Si-4000 and calibrated using nitrogen adsorption data for several large-pore MCM-41 silicas, as described elsewhere.[11] This t curve is accurately approximated in the relative pressure range from 0.1 to 0.95 by the following empirical equation:[11]

$$t(p/p_0)\ [\text{nm}] = 0.1\left[\frac{60.65}{0.03071 - \log[p/p_0]}\right]^{0.3968} \tag{3}$$

The BJH primary mesopore diameter, w_{BJH}, was defined as the pore size corresponding to the maximum of the differential pore size distribution.

To verify the validity of the t curve for the reference silica gel (approximated by eq 3), the nitrogen statistical film thickness on the MCM-41 surface (expressed as a function of the relative pressure and denoted as $t_{MCM-41}(p/p_0)$) was evaluated on the basis of the following equation,[11]

$$t_{MCM-41}(p/p_0) = \frac{w_d}{2}\left[1 - \left(\frac{v_{p,max} - v_p(p/p_0)}{v_{p,max}}\right)^{1/2}\right] \tag{4}$$

where $v_p(p/p_0)$ is the adsorbed amount in primary mesopores as a function of relative pressure:

$$v_p(p/p_0) = v(p/p_0) - \frac{S_{ex}}{S_{BET,ref}}v_{ref}(p/p_0) \tag{5}$$

In eq 5, $v(p/p_0)$ is the adsorbed amount for a given MCM-41 sample as a function of relative pressure, S_{ex} is the external surface of the sample, and $S_{BET,\,ref}$ and $v_{ref}(p/p_0)$ are the BET specific surface area and the adsorbed amount as a function of relative pressure, respectively, for the reference adsorbent used in calculations of the external surface area. The maximum adsorbed amount in primary mesopores was assumed to be equal to the adsorbed amount in primary mesopores at the relative pressure of 0.85. Further details of calculations of statistical film thickness curves for MCM-41 materials can be found elsewhere.[11]

Results and Discussion

X-ray Diffraction Spectra. Powder X-ray diffraction (XRD) spectra for the MCM-41 materials under study are shown in Figure 1 and (100) interplanar spacing values are listed in Table 1. The XRD patterns indicate that the samples exhibited hexagonal structures with a high degree of structural ordering, since all of the spectra featured narrow (100) peaks and, in most cases, well-separated (110) and (200) reflections. Only for MCM-41-16B were the (110) and (200) peaks somewhat less pronounced. XRD spectra for samples MCM-41-16A, -18, and -16C also featured clear (210) and (300) reflections. The presence of the (300) peak for MCM-41-16C is noteworthy, since large-unit-cell MCM-41 materials ($d_{100} > 5$ nm) usually exhibit a lower degree of structural ordering than the samples with smaller unit cell dimensions. Only large-pore MCM-41 materials prepared using mixtures of alkyltrimethylammonium surfactants and gemini or divalent surfactants were reported to exhibit more than four XRD reflections[2] and samples synthesized in the presence of docosyltrimethylammonium surfactants were shown to feature four pronounced peaks on their XRD

(13) Kruk, M.; Jaroniec, M.; Ryoo, R.; Kim, J. M. *Microporous Mater.* **1997**, *12*, 93.

(14) Sing, K. S. W.; Everett, D. H.; Haul, R. A. W.; Moscou, L.; Pierotti, R. A.; Rouquerol, J.; Siemieniewska, T. *Pure Appl. Chem.* **1985**, *57*, 603.

(15) Kruk, M.; Jaroniec, M.; Sayari, A. *Chem. Mater.* **1999**, *11*, 492.

(16) Barrett, E. P.; Joyner, L. G.; Halenda, P. P. *J. Am. Chem. Soc.* **1951**, *73*, 373.

Table 1. Structural Parameters of MCM-41 Samples under Study[a]

sample	d_{100} (nm)	S_{BET} (m^2/g)	V_t (cm^3/g)	S_{ex} (m^2/g)	V_p (cm^3/g)	w_d (nm)	b_d (nm)	w_{BJH} (nm)
12	3.44	880	0.66	50	0.54	3.08	0.89	3.07
16A	4.17	900	0.90	100	0.65	3.88	0.94	3.85
18	4.51	860	0.93	110	0.67	4.22	0.99	4.16
16B	5.04	640	0.66	60	0.56	4.55	1.27	4.66
16C	5.37	720	0.81	50	0.72	5.11	1.09	5.12

[a] d_{100}, XRD (100) interplanar spacing; S_{BET}, BET specific surface area; V_t, total pore volume; S_{ex}, external surface area; V_p, primary mesopore volume; w_d and b_d, primary mesopore diameter and pore wall thickness calculated using geometrical considerations (eq 1); w_{BJH}, maximum of the pore size distribution calculated using the BJH method with the corrected form of the Kelvin equation (eq 2) and the *t* curve approximated by eq 3.

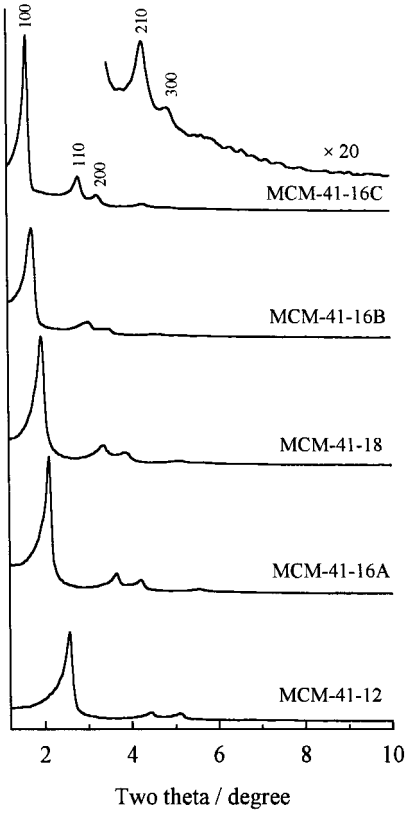

Figure 1. Powder X-ray diffraction patterns for the MCM-41 samples.

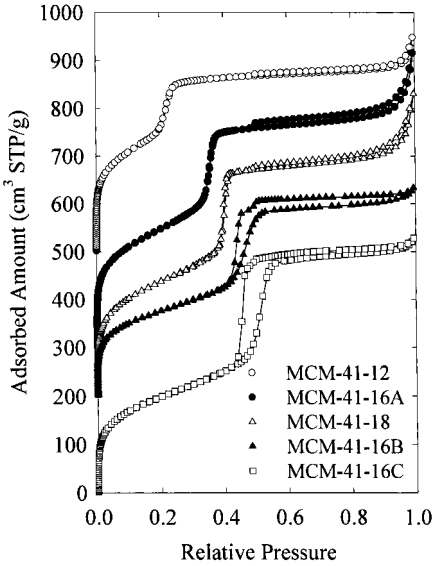

Figure 2. Nitrogen adsorption isotherms for the MCM-41 samples. The isotherms for MCM-41-12, -16A, -18, and -16B were shifted by 500, 300, 200, and 200 cm^3 STP/g, respectively.

spectra.[17] So MCM-41-16C probably exhibits the highest structural ordering among the reported large-unit-cell MCM-41 materials prepared using common alkyltrimethylammonium surfactants, such as hexadecyltrimethylammonium.[7−10] The mechanism of formation of these large-pore materials was discussed elsewhere.[9,18,19] The current results also demonstrated that application of the pH adjustment procedure[12,13,20] is suitable for the preparation of excellent quality materials templated by octadecyltrimethylammonium and dodecyltrimethylammonium surfactants.

Nitrogen Adsorption Isotherms. It can be seen in Figure 2 that nitrogen adsorption isotherms for the MCM-41 samples under study featured narrow steps of capillary condensation in primary mesopores, which indicates high pore size uniformity. As the (100) interplanar spacing of the materials increased from 3.4 to 5.4 nm (see Table 2), the position of this step shifted to higher relative pressures (from 0.22 to 0.51). For samples MCM-41-16A and -18, which exhibited capillary condensation at a relative pressure of about 0.4, which corresponds to the pore size of about 4 nm, the steps on adsorption isotherms were particularly narrow. MCM-41 samples with very sharp condensation steps located at similar relative pressure values have already been reported,[4,13,21,22] whereas the capillary condensation steps observed at relative pressures significantly lower or higher than 0.4 were usually significantly broader. This indicates that the highest degree of structural ordering can be attained for MCM-41 materials with the pore size of about 4 nm when cetyltrimethylammonium or octyltrimethylammonium surfactants are used as templates. Other surfactants or their mixtures were shown to be suitable for the synthesis of highly ordered MCM-41 samples with different pore sizes.[2,17]

In the case of MCM-41-12 and -16A, the capillary condensation in primary mesopores was not accompanied with hysteresis, but for MCM-41-18, the desorption branch did not follow the adsorption branch of the isotherm and a very narrow triangular hysteresis loop was observed. The adsorption isotherm for sample MCM-41-16B exhibited a pronounced triangular hysteresis loop with a very steep desorption branch. The isotherm for sample MCM-41-16C had a hysteresis loop of shape intermediate between a triangular one and one with parallel adsorption

(17) Namba, S.; Mochizuki, A.; Kito, M. *Stud. Surf. Sci. Catal.* **1998**, *117*, 257.
(18) Sayari, A.; Kruk, M.; Jaroniec, M.; Moudrakovski, I. L. *Adv. Mater.* **1998**, *10*, 1376.
(19) Kruk, M.; Jaroniec, M.; Sayari, A. *J. Phys. Chem. B* **1999**, *103*, 4590.
(20) Ryoo, R.; Jun, S. *J. Phys. Chem. B* **1997**, *101*, 317.
(21) Cheng, C.-F.; Park, D. H.; Klinowski, J. *J. Chem. Soc., Faraday Trans.* **1997**, *93*, 193.
(22) Sonwane, C. G.; Bhatia, S. K. *Chem. Eng. Sci.* **1998**, *53*, 3143.

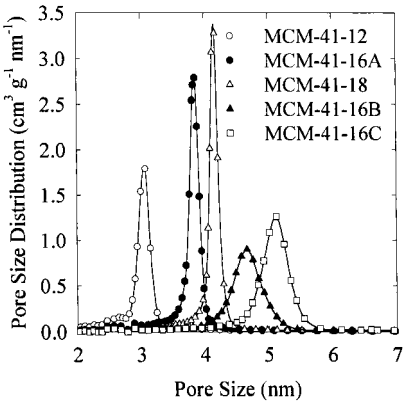

Figure 3. BJH pore size distributions for the MCM-41 silicas.

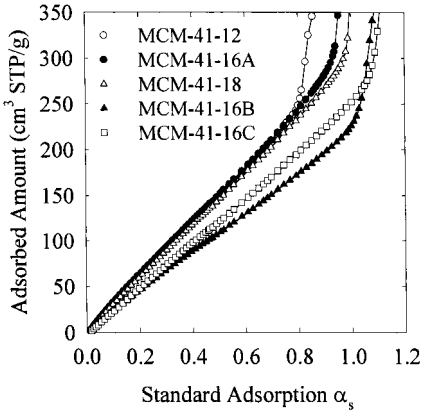

Figure 4. Low-pressure parts of a_s plots for the MCM-41 samples.

and desorption branches. In this case, the desorption branch was also much steeper than the adsorption branch. A gradual development of hysteresis loops and the change in their shape is consistent with a previous study[11] and can be explained as a result of the increasing primary mesopore size for the MCM-41- materials in the following order: -12 < -16A < -18 < -16B < -16C.

One can also notice that hysteresis loops related to capillary condensation in secondary mesopores extend in a wide range of pressures. For samples MCM-41-12, -16A, and -18, these hysteresis loops were clearly separated from the region of capillary condensation in primary mesopores and their lower closure points were located at relative pressures of about 0.48. In the case of samples MCM-41-16B and -16C, hysteresis loops related to adsorption in primary and secondary mesopores were not fully separated, but it can be seen that capillary evaporation from secondary mesopores was completed at a relative pressure of about 0.48, which is distinctly different, especially for MCM-41-16B, from the pressure of capillary evaporation in primary mesopores of these samples. It should be noted that capillary condensation in secondary mesopores takes place at relative pressures close to saturation (above 0.8) and thus the width of these pores is at least several times larger than that of the primary mesopores.

Mesopore Size Distributions. As can be seen in Figure 3, the MCM-41 samples under study exhibit narrow pore size distributions (PSDs). PSDs are remarkably narrow in the case of samples MCM-41-16A and -18, which exhibit pore sizes of about 4 nm. The PSDs for the materials with both larger and smaller pores are much broader. The width of the pore size distribution for MCM-41 can be related to two factors. One of them is the heterogeneity of the average diameter of different channels in the structure. The second one is variation of the channel diameter along single channels. It was suggested[11] that, for the MCM-41 materials, which exhibit adsorption−desorption hysteresis, the width of the hysteresis loop is related primarily to the second factor mentioned above. However, it is difficult to draw some conclusions about the nature of pore size distribution broadening for the samples under study, since adsorption isotherms for MCM-41-12 and -16A exhibit no hysteresis, and in the case of the MCM-41-18, -16B, and -16C samples, hysteresis loops are necessarily relatively narrow because of the fact that they are located close to the lower pressure limit of occurrence of hysteresis loops. Thus, on the basis of nitrogen adsorption data alone, it is difficult to elucidate the nature of the broadening of pore size distributions for the MCM-41 samples under study. It should also be noted that the PSDs reported herein were calculated using adsorption branches of isotherms, whereas many PSDs previously reported were obtained on the basis of desorption data, which might have led to artificial narrowing of these PSDs, as discussed elsewhere.[11]

Comparative Plots. Shown in Figure 4 are low-pressure parts of a_s plots for the MCM-41 materials under study. In all cases, the initial parts of the plots were found to be linear starting from $a_s = 0$. This behavior suggests the absence of detectable amounts of micropores. The deviations from linearity at $a_s \geq 0.8$ can be attributed to capillary condensation in primary mesopores.

Structural Parameters. Higher-pressure parts of a_s plots were used to evaluate external surface areas and primary mesopore volumes for the samples. These quantities, along with BET specific surface areas and total pore volumes, are listed in Table 1. The MCM-41 samples under study exhibited rather moderate values of the BET specific surface area (below or equal to 900 m^2/g) and primary mesopore volume (below 0.75 cm^3/g). Samples MCM-41-16A and -18 were found to have appreciable external surface areas and secondary mesopore volumes (that is, differences between the total pore volumes and primary mesopore volumes) equal to about 100 m^2/g and 0.25 cm^3/g, respectively.

The primary mesopore size, w_d, and the pore wall thickness, b_d, for the MCM-41 samples under study were evaluated from the interplanar spacings and primary mesopore volumes on the basis of geometrical considerations (eq 1). The primary mesopore size, w_{BJH}, was also evaluated using the BJH method[16] with the corrected form of the Kelvin equation for nitrogen adsorption in cylindrical pores (eqs 2 and 3).[11] It can be seen that the two methods of evaluation of the primary mesopore diameter provided results differing by at most 0.11 nm, which is a remarkably good agreement, especially when one takes into account that the adsorption and/or XRD data may be inaccurate to some extent. It is also noteworthy that the materials under study, and MCM-41-16B and -16C in particular, exhibit rather thick pore walls in comparison to many other MCM-41 samples[8,13] (in comparing pore wall thicknesses, it is essential to use the same evaluation method, since results may differ widely depending on the choice of the latter[15]). The formation of thick pore walls was noted in ref 9, which reported the procedure used for the preparation of MCM-41-16B and -16C. For a sample prepared at 438 K for 2 days (the same conditions as those for MCM-41-16B), the (100) interplanar spacing of 5.5 nm and the specific surface area of 760 m^2/g were reported, which are in good agreement with our data (Table 1). However, the pore walls of this material were claimed to be as thick as 2.7 nm, which was already suggested to be

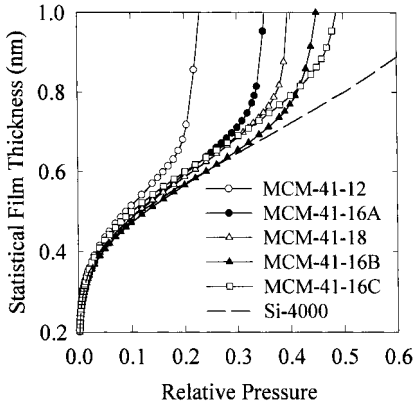

Figure 5. Comparison of statistical film thickness curves calculated for the MCM-41 samples under study with the statistical film thickness curve for a macroporous silica gel LiChrospher Si-4000.[11]

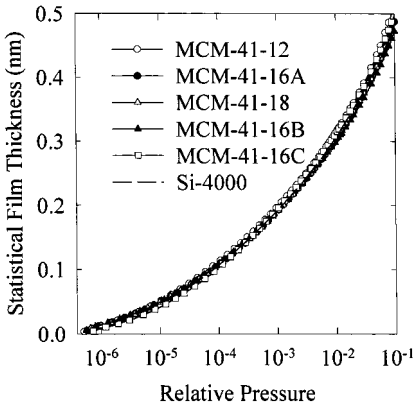

Figure 6. Comparison of low-pressure parts of statistical film thickness curves calculated for the MCM-41 samples under study with the statistical film thickness curve for a macroporous silica gel LiChrospher Si-4000.[11]

unrealistic,[5,15] and the pore size was estimated to be only 3.6 nm. Our current study indicates the pore size of 4.6 nm and the pore wall thickness of 1.3 nm for the material prepared in the same conditions, thus confirming that the pore wall thickness reported in ref 9 was overestimated and the pore size was underestimated, as suggested before.[5,15,19]

Statistical Film Thickness Curves. Shown in Figures 5 and 6 are nitrogen statistical film thickness curves (*t* curves) for the MCM-41 materials under study. Low-pressure parts of the *t* curves were very similar for all samples (see Figure 6), and also similar to the *t* curve derived previously for a macroporous silica gel, LiChrospher Si-4000.[11] It is interesting that, in the low-pressure region, the film thickness at given pressure values tends to increase as the pore size decreases, being the highest for MCM-41-12 and the lowest for MCM-41-16C. Similar differences in the low-pressure adsorption behavior have already been reported for MCM-41 materials with pore sizes from 2.8 to 3.8 nm and were suggested to result primarily from increased pore wall curvature, and consequently, enhanced interactions of nitrogen molecules with the pore walls as the pore size decreases.[23] MCM-41-16B does not exhibit the same behavior as the other MCM-41 samples under study, which may possibly result from a somewhat different structure of the former. Namely, sample MCM-41-16B exhibits pronounced triangular hysteresis loop at higher relative pressures (above about 0.5), indicating a possibility of the presence of a small amount of disordered nonmesostructured domains in the calcined material.[15] Indeed, MCM-41-16B was the only sample among those analyzed here for which the primary mesopore size assessed using the BJH method with the corrected Kelvin equation (eq 3) was noticeably larger (by 0.11 nm) than the pore diameter assessed on the basis of geometrical considerations (eq 1). Such a behavior was recently predicted to indicate the presence of disordered nonmesostructured domains in calcined MCM-41, but since its magnitude is very small for MCM-41-16B, it may actually be insignificant.

As was mentioned above, the *t* curves derived for MCM-41 samples under study exhibited a good agreement in the low-pressure range with the *t* curve for a macroporous silica gel. This is essentially because of the nonmicroporous and siliceous nature of these materials. However, one can expect differences at higher pressures, where capillary condensation in the primary mesopores of MCM-41 takes place. This was actually found to be the case. The *t* curve for MCM-41-12 started to exhibit pronounced upward deviations at a relative pressure of about 0.1, which is significantly below the onset of capillary condensation (about 0.2). In the case of the other MCM-41 samples, the increases in the statistical film thickness (with respect to the film thickness for the macroporous silica) also preceded the capillary condensation. It cannot be precluded that such a behavior resulted from the presence of a small fraction of pores with diameters appreciably smaller than the average pore size. However, it is more likely that (i) the adsorbed film formation on pore walls is enhanced to some extent before the capillary condensation takes place, for instance, because of a relatively small diameter of the inner part of the pore, which is still unoccupied by the adsorbed molecules, and/or (ii) MCM-41 pores may exhibit some variation of their diameter along the main pore axis. These two factors probably account for the increase in *t* curves below the onset of capillary condensation, but further studies would be needed to fully explain the observed phenomenon. Anyway, it is clear that, below the capillary condensation region, *t* curves for MCM-41 materials with pore sizes above 3 nm are satisfactorily approximated by the *t* curve for the macroporous silica. This indicates that mesopore size distribution calculations based on the *t* curve for a proper reference adsorbent, such as those used in the BJH method, are inherently capable of providing good estimations of PSDs despite their approximate character, if only a proper relation between the pore size and capillary condensation pressure is known. Such a relation for cylindrical pores was recently reported[11] and is described by eqs 2 and 3.

It is noteworthy that the *t* curve for MCM-41-16B differed slightly from those for the other MCM-41 materials, which may possibly be due to a somewhat different structure of the material. Moreover, there is a possibility of inaccuracy in the *t* curve evaluation since the latter depends on accurate estimation of the primary mesopore diameter using geometrical considerations of a purely hexagonal structure. As discussed above, there is a possibility of the presence of a small amount of disordered domains in the structure of MCM-41-16B, which would make the pore size estimation less accurate. It also should be noted that application of the primary mesopore size evaluated using the properly calibrated BJH method instead of the geometrical formula (eq 1) in the *t* curve calculations for MCM-41-16B would increase the obtained statistical film thickness by 2.4%, thus improving the

(23) Kruk, M.; Jaroniec, M.; Sayari, A. *J. Phys. Chem. B* **1997**, *101*, 583.

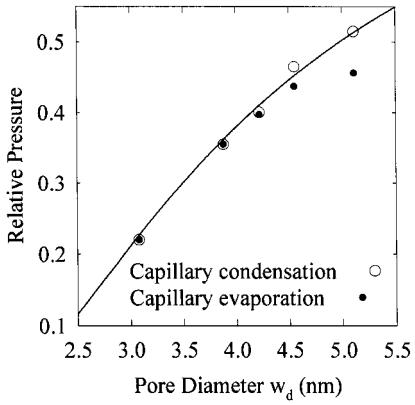

Figure 7. Comparison of the relation between the capillary condensation/evaporation pressure and the primary mesopore size for MCM-41 samples under study with the recently reported[11] relation between the capillary condensation pressure and the pore size.

agreement between high-pressure parts of the *t* curves for MCM-41 materials.

Comparison of the Current Results with Predictions Based on the Corrected Kelvin Equation. Shown in Figure 7 are capillary condensation and capillary evaporation pressures as functions of the primary mesopore diameter for the MCM-41 materials. The capillary condensation pressures increased smoothly (within experimental error) as the pore diameter increased, which is in agreement with the recently reported study.[11] The increase in capillary evaporation pressure was relatively small in the range of pore sizes from about 4.2 to 5.1 nm, once again supporting previously reported results.[11] As can be seen in Figure 7, the corrected Kelvin equation for adsorption in cylindrical pores[11] provides a very accurate estimation of capillary condensation pressures for highly ordered MCM-41 materials, which strongly supports the applicability of the latter equation in calculations of pore size distributions, especially for MCM-41 and other ordered mesoporous silicas.

Conclusions

The current work demonstrated that highly ordered MCM-41 silicas with pore sizes up to about 5.1 nm can be prepared using common alkyltrimethylammonium surfactants by employing the repeated pH adjustment or high-temperature synthesis procedures. Adsorption studies of these high-quality model materials confirmed the validity of the recently proposed corrected form of the Kelvin equation for nitrogen adsorption in cylindrical pores. The obtained statistical film thickness curves for MCM-41 were found to be in agreement with the recently derived *t* curve for a macroporous silica, especially in the low-pressure range, but it was observed that the onset of capillary condensation in primary mesopores was preceded by an increase in the statistical film thickness in comparison to that for the macropore surface. This increase was relatively small for the samples under study (pore diameter above 3 nm). Therefore, in the case of nitrogen at 77 K, the adsorption process in cylindrical siliceous mesopores (at least those of the size above 3 nm) can be adequately approximated as a formation of a multilayer of the thickness similar to that on the macroporous reference adsorbent (for instance, described by eq 3), which is followed by capillary condensation at pressures described by the corrected Kelvin equation (described by eq 2). Thus, one can expect that methods of calculation of mesopore size distributions based on the *t* curve for a proper macroporous reference (such as the BJH method) should provide good results, provided a correct relation between the pore size and the capillary condensation pressure is used.

Acknowledgment. The donors of the Petroleum Research Fund administrated by the American Chemical Society are gratefully acknowledged for support of this research.

LA990179V